


New hybrid between NSGA-III with multi-objective particle swarm optimization to multi-objective robust optimization design for Powertrain mount system of electric vehicles

Advances in Mechanical Engineering
2020, Vol. 12(2) 1–14
© The Author(s) 2020
DOI: 10.1177/1687814020904253
journals.sagepub.com/home/ade


Nguyễn Huy Trường¹ and Dinh-Nam Dao² 

Abstract

In this study, a new methodology, hybrid NSGA-III with multi-objective particle swarm optimization (HNSGA-III&MOPSO), has been developed to design and achieve cost optimization of Powertrain mount system stiffness parameters. This problem is formalized as a multi-objective optimization problem involving six optimization objectives: mean square acceleration and mean square displacement of the Powertrain mount system. A hybrid HNSGA-III&MOPSO is proposed with the integration of multi-objective particle swarm optimization and a genetic algorithm (NSGA-III). Several benchmark functions are tested, and results reveal that the HNSGA-III&MOPSO is more efficient than the typical multi-objective particle swarm optimization, NSGA-III. Powertrain mount system stiffness parameter optimization with HNSGA-III&MOPSO is simulated, respectively. It proved the potential of the HNSGA-III&MOPSO for Powertrain mount system stiffness parameter optimization problem. The amplitude of the acceleration of the vehicle frame decreased by 22.8%, and the amplitude of the displacement of the vehicle frame reduced by 12.4% compared to the normal design case. The calculation time of the algorithm HNSGA-III&MOPSO is less than the algorithm NSGA-III, that is, 5 and 6 h, respectively, compared to the algorithm multi-objective particle swarm optimization.

Keywords

NSGA-III algorithm, multi-objective particle swarm optimization algorithm, optimal solution, Powertrain mount system stiffness, multi-objective evolutionary algorithms, mounting system

Date received: 16 April 2019; accepted: 3 January 2020

Handling Editor: Yunn-Lin Hwang

Introduction

Due to the different configuration and operating principle of electric motor and internal combustion engine (ICE), the speed and speed of electric motors and ICEs vary greatly, so the dynamic characteristics on electric vehicles will be very different from traditional ICE cars. On the other hand, due to increasing environmental requirements, the big trend is shifting to a dynamical system that uses electricity instead of gasoline as currently. Therefore, our research focuses on the vibration of electric motors in vehicles. The electric vehicle's

drive system consists of Powertrain, transmission, and clutch, which is the source of energy for the vehicle and is also one of the major sources of vibration in the car.

¹Institute of Military Mechanical Engineering, Hanoi, Vietnam

²Control Technology College, Le Quy Don Technical University, Hanoi, Vietnam

Corresponding author:

Dinh-Nam Dao, Control Technology College, Le Quy Don Technical University, Hanoi 100000, Viet Nam.
Email: daodinhnamk@gmail.com



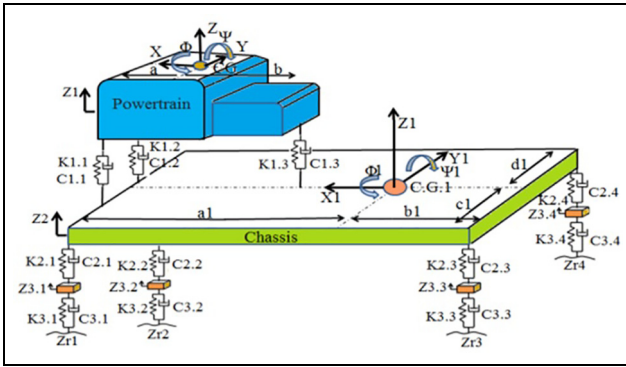


Figure 1. A full-car dynamic model with a Powertrain mount system.

There have been some authors studying electric vehicle power systems.¹⁻³ Therefore, to isolate vibrations transmitted from the transmission system to the vehicle body, the Powertrain mount is usually installed between the transmission and the vehicle body.⁴ Powertrain mounting system is a system mounted between the frame and the Powertrain. These mounts play an important role in the entire dynamic system of the vehicle and the principle diagram of the full-car dynamic model with the Powertrain mount system is shown in Figure 1. Powertrain mounting system has a suitable stiffness. On the one hand, it will improve the noise, vibration performance, and harshness of the vehicle; on the other hand, it will extend the life of the Powertrain and related parts.⁵ If calculated according to the characteristics of controllability, Powertrain racks can be classified into passive Powertrain racks (hydraulic and rubber racks are the most popular), Powertrain racks, and sold Powertrain. Typically, a rubber hanger consists of a metal frame in which the rubber is bonded through adhesives or during vulcanization. With the advantage of low cost and simple structure, rubber suspension is the most widely used engine mount. The important step to designing racks is the parameters that match their stiffness. Suitable rigidity can not only reduce the vibration of the Powertrain to the elastic platform (such as frame and body) but can also reduce the unwanted impact of excitation from the road and impact wheel on the body. One of the most important steps to designing Powertrain racks is to calculate the stiffness parameters of the suspension so that it is best suited to the Powertrain and chassis parameters. With the stiffness parameters of the appropriate Powertrain mount, it can not only reduce the vibration of the Powertrain to the chassis but also reduce the undesirable effects of stimuli from the road and movable impact wheels transfer on the body. By that, the problem of calculating the optimal hardness parameters for the Powertrain mounting system is an important task in designing the vehicle's dynamic

system. This is a multi-object concurrency optimization problem.

Recently, a number of researchers have studied in the field of multi-objective optimization. They introduced various methods, among them, presented in Konak et al.⁶ in reviews and guidelines. NSGA-II algorithm is published by Deb et al.⁷ and so far there are a number of variations and applications of NSGA II algorithm developed by Chang and Chang,⁸ Ishibuchi et al.,⁹ and Malekmohammadi et al.¹⁰ Deb and Jain¹¹ have published and applied the MONGA-II method for a number of multi-objective testing problems. NSGA-III algorithms have been studied to face multiple goals at once (more than two). This is the Algorithm published by Deb and Jain¹² in 2014, in which they changed some selection mechanisms. They came up with a multi-objective evolution algorithm based on reference points based on the NSGA-II algorithm. They mainly emphasize that population members are not popular, but close to the combination of a set of reference points provided. The NSGA-III algorithm is proposed to apply to a number of multi-objective testing problems with 3 to 15 goals.

In addition, there are some researchers studying the optimal problem of many objects. They have studied and developed multi-objective particle swarm optimization (MOPSO) algorithm. MOPSO algorithm is one of the most popular multi-objective optimization algorithms conceptually; it is similar to particle swarm optimization (PSO). Coello et al.¹³ and his colleagues applied MOPSO algorithm to handle multiple objectives. In recent studies of MOPSO algorithm,¹³⁻¹⁵ they have shown additional conditions such as multiple estimates used to achieve better exploration characteristics. Baltar and Fontane^{16,17} improved the MOPSO algorithm to minimize deviation from outflow water quality. They also published an application of an evolutionary optimization algorithm for multi-objective analysis for reservoir operations and planning. Reddy and Kumar^{18,19} published and applied the Elitist-Mutated operator with MOPSO (EM-MOPSO) to show the reduction of total squared deviations for irrigation, maximizing the yield of aquatic electricity and the degree of satisfaction of downstream water quality requirements. In addition, they used the Elitist-Mutated MOPSO algorithm (EM-MOPSO) to maximize hydropower production and minimize the total number of squares to release annual irrigation from demand. Wang et al.²⁰ have applied modified MOPSO to minimize the highest water level, release peak flow, water level difference after flood season, and flood control level. In this case, the concept of Pareto dominance for selecting leaders from a non-dominated external archive has been utilized by MOPSO algorithm where the leaders of swarms that guide the particles to the

Pareto Frontier are selected from the top portion of the archive at each iteration.

Recently, there are some new optimization algorithms proposed.²¹⁻²⁷ However, each algorithm has advantages and disadvantages, precisely, because no algorithm can solve all optimization problems correctly. Therefore, new hybrid algorithms should be proposed to be able to solve new problems that have not been resolved before and/or have better accuracy than existing techniques.

On the other hand, there are some hybrid methods of optimization algorithms that have been recently developed: Jeong et al.²⁸ published the development and investigation of the GA/PSO-hybrid algorithm effectively for optimizing the design in the real world. Premalatha and Natarajan²⁹ published hybrid PSO and GA for Global Maximization. A multi-objective particle optimization method based on extreme optimization with variable and inertial inertia mutations (HM-TVWF-MOEPSO) has been proposed to solve some of the problems in optimization, multi-purpose particle chemistry, and improved algorithm performance.³⁰ A new hybrid heuristic algorithm is published in the current work for multi-objective optimization issues. The hybrid algorithm has proposed a method to combine the simple algorithm Nelder-Mead with the non-dominant genetic algorithm II (NSGA II) to find the best global point. The performance of this new algorithm has been presented through a number of complex benchmark functions.³¹ A pre-selected pre-creation method has been published to address multivariate technical optimization problems.³² This method can set the number of Pareto solutions and optimize multiple times until satisfactory results are obtained. This is an effective algorithm that consists of independent parallel genetic algorithms by dividing the entire population into multiple populations,³³ in which each population group will be assigned to different weights to search for optimal solutions in different directions. Therefore, most published hybrid algorithms have many advantages. This breeding has overcome the limitations of each optimization algorithm. This proves that this is one of the methods that should be studied in multi-objective optimization.

In this article, a new hybrid optimization algorithm is proposed in this work for multi-objective problems. This is the hybrid between the MOPSO algorithm and a multi-objective genetic algorithm (NSGA-III) to find the best of the Pareto optimal front. HNSGA-III&MOPSO is proposed to outperform MOPSO and NSGA-III because it uses a combination of search operators of both algorithms to create a new population. This makes the search process more diverse, wider search space. New hybrid algorithms show better performance than other algorithms. This is demonstrated through a number of complex benchmarking functions

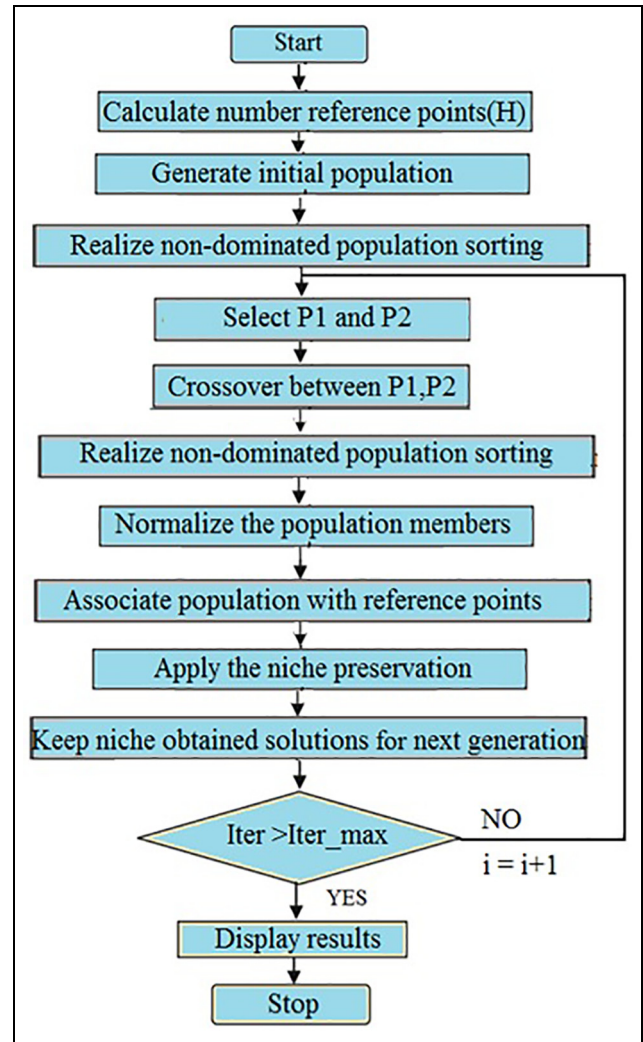


Figure 2. Flow chart of NSGA-III.

and Powertrain mount system stiffness parameter optimization problem with six-objective optimization in a three-dimensional (3D) model. The amplitude of the acceleration of the vehicle frame decreased by 22.8%, and the amplitude of the displacement of the vehicle frame reduced by 12.4% compared to the normal design case. The calculation time of the algorithm HNSGA-III&MOPSO is less than the algorithm NSGA-III, that is, 5 and 6 h, respectively, compared to the algorithm MOPSO.

The organization of this article is as follows. Section “Structure” describes the proposed hybrid HNSGA-III&MOPSO method and computational experimentation with several benchmark functions. Section “Vibration characteristic of the Powertrain mount system” describes the vibration characteristic of the Powertrain mount system and simulation results of application HNSGA-III&MOPSO method to optimization of the Powertrain mount system stiffness

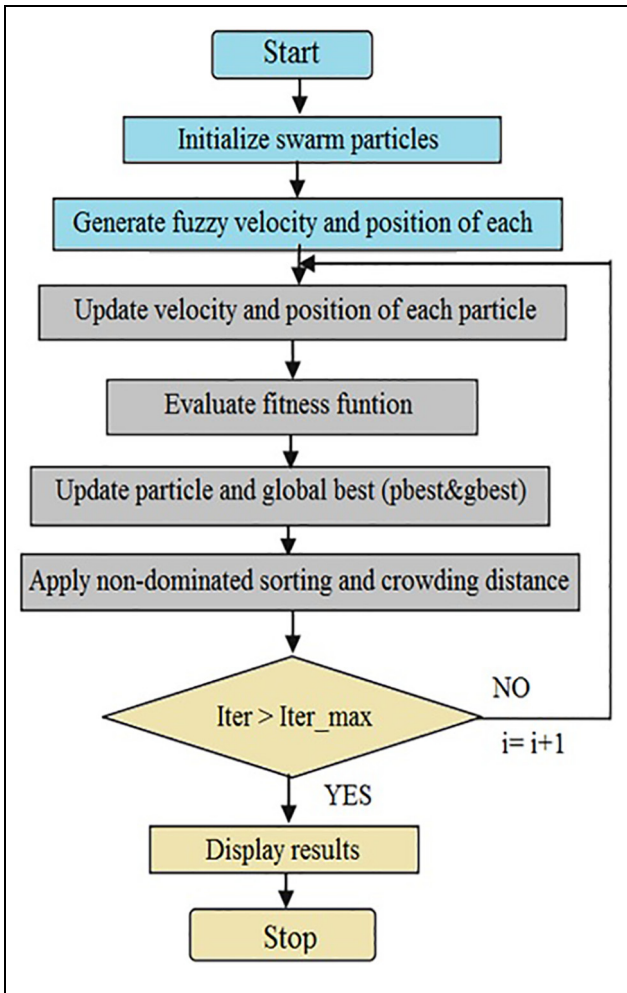


Figure 3. Flow chart of MOPSO.

parameter. The final section “Conclusion” concludes the article.

Structure

Genetic algorithm NSGA-III

This algorithm was published by Deb and Jain¹² in 2014 with a number of change mechanisms selected. NSGA-III algorithm is based on the steps described in Figure 2.

PSO (MOPSO)

Kennedy et al.³⁴ published an algorithm based on the basis of PSO algorithm for optimization. They improved the PSO algorithm to find the Pareto optimal front. Therefore, the improved PSO algorithm is suitable to optimize many goals with high convergence speed, allowing each individual to benefit from the experience. A diagram of MOPSO is shown in Figure 3.

Hybrid NSGA-III and MOPSO (HNSGA-III&MOPSO)

Each evolutionary algorithm has different strengths and characteristics. Therefore, it is only natural to think of integrating different algorithms to handle a complex problem. In the field of research, the evolution algorithm integrates two or more optimization algorithms into a single frame. The results show that hybrid algorithms have higher efficiency because they can exchange characteristics to improve the disadvantages and enhance their advantages. Parallel hybridization can improve exploration and exploitation which can yield higher performance and more favorable conditions than any single algorithm. These population-based approaches use different techniques to explore the search space and, when they are combined, will improve the trade-off between exploration and exploitation tasks to converge around. The best solution was possible.

HNSGA-III&MOPSO hybrid approach. HNSGA-III&MOPSO is implemented in parallel breeding; that is, the initial population will be generated in both NSGA-III and MOPSO. After that, two separate populations will be mixed together. The new population after combining will be both algorithms used as their own population to perform fitness function calculations that evaluate the evolution of each algorithm. By the next generation, the new population created by the two algorithms is mixed together to form a common population. The process repeats until the end of evolution condition is completed. The process of parallel operation is to create an extremely diverse and widespread population. This makes the algorithm have a wide search strategy across the regions, besides making the process more convergent. Therefore, the analysis time is reduced and the results are more accurate.

The pseudo code of the proposed algorithm:

Parameter initialization for NSGA-III and MOPSO algorithms.

MOPSO algorithms: Swarm population initialization.

NSGA-III algorithms: GA population initialization.

While travel not completed.

Combination the two populations.

MOPSO algorithm.

While sub-travel not completed.

Determined fitness function.

Set P_{best} and G_{best} .

Update particle velocity v_i^{k+1} and position x_i^k .

Proceed non-dominated sorting and crowding distance.

End while.

NSGA-III algorithm.

While evolution not completed.

Choose two parents $P1$ and $P2$ using the tournament method.

(continued)

Proceed the crossover between $P1$ and $P2$ with a probability P_c .
 Recognize the non-dominated population sorting.
 Normalize the population members.
 Associate the population member with the reference Points.
 Apply the niche preservation (counter).
 Keep the appropriate solutions obtained for the next generation.
 End while.
 End while.

benchmarks that are published in CEC 2009,³⁵⁻³⁸ listed in Table 1. The results are compared to algorithms of NSGA-III and MOPSO. For the performance metric,²² Inverted Generational Distance (IGD),³⁹ Spacing (SP), and Maximum Spread (MS)⁴⁰ criteria are employed to measure convergence, quantity, and coverage, respectively. The mathematical formulation of IGD is as follows

$$IGD = \frac{\sqrt{\sum_{i=1}^N d_i^2}}{N} \quad (1)$$

A flow chart of HNSGA-III&MOPSO is shown in Figure 4.

Computational experimentation with several benchmark functions

Numerical results. In this section, the performance of HNSGA-III& MOPSO is evaluated using five

where N is the number of true Pareto optimal solutions and d_i indicates the Euclidean distance between the i th true Pareto optimal solution and the closet obtained Pareto optimal solutions in the reference set. It should be noted that $IGD = 0$ indicates that all members of the non-dominated solutions are in the true Pareto Front

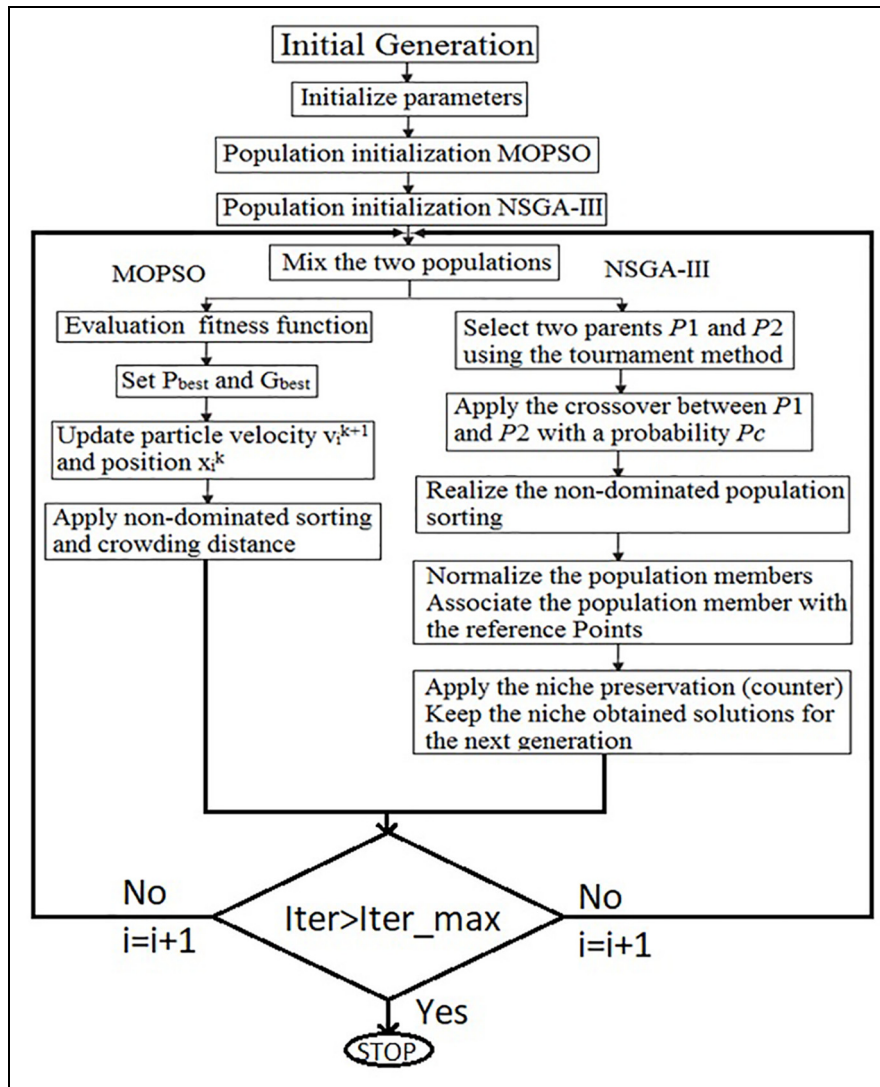


Figure 4. Flow chart of HNSGA-III&MOPSO.

Table 1. Benchmark functions for test multi-objective optimization.

Mathematics formulation	Mathematics formulation	Mathematics formulation
<p>UF2:</p> $f_1 = x_1 + \frac{2}{ J_1 } \sum_{j \in J_1} y_j^2$ $f_2 = 1 - \sqrt{x} + \frac{2}{ J_2 } \sum_{j \in J_2} y_j^2$ $y_j = \begin{cases} x_j = \left[0.3x_1^2 \cos\left(24\pi x_1 + \frac{4j\pi}{n}\right) + 0.6x_1 \right] \sin\left(6\pi x_1 + \frac{j\pi}{n}\right) \text{if } j \in J_1 \\ x_j = \left[0.3x_1^2 \cos\left(24\pi x_1 + \frac{4j\pi}{n}\right) + 0.6x_1 \right] \sin\left(6\pi x_1 + \frac{j\pi}{n}\right) \text{if } j \in J_2 \end{cases}$ <p>$J_1 = \{j j \text{ is odd and } 2 \leq j \leq n\}$; $J_2 = \{j j \text{ is even and } 2 \leq j \leq n\}$;</p>	<p>UF4:</p> $f_1 = x_1 + \frac{2}{ J_1 } \sum_{j \in J_1} h(y_j)$ $f_2 = 1 - x_2 + \frac{2}{ J_2 } \sum_{j \in J_2} h(y_j)$ $y_j = x_j - \sin\left(6\pi x_1 + \frac{j\pi}{n}\right)$ <p>$j = 2, 3, \dots, n$</p> $h(t) = \frac{ t }{1 + e^{2 t }}$ <p>J_1 and J_2 are the same as those of UF2</p>	<p>UF5:</p> $f_1 = x_1 + \left(\frac{1}{2N} + \varepsilon\right) \sin(2N\pi x_1) + \frac{2}{ J_1 } \sum_{j \in J_1} h(y_j)$ $f_2 = 1 - x_1 + \left(\frac{1}{2N} + \varepsilon\right) \sin(2N\pi x_1) + \frac{2}{ J_2 } \sum_{j \in J_2} h(y_j)$ $y_j = x_j - \sin\left(6\pi x_1 + \frac{j\pi}{n}\right)$ <p>$j = 2, 3, \dots, 4$</p> $h(t) = 2t^2 - \cos(4\pi t) + 1$ <p>J_1 and J_2 are the same as those of UF2, $\varepsilon > 0$.</p>
<p>UF8:</p> $f_1 = \cos(0.5x_1\pi) \cos(0.5x_2\pi) + \frac{2}{ J_1 } \sum_{j \in J_1} \left(x_j - 2x_2 \sin\left(2\pi x_1 + \frac{j\pi}{n}\right) \right)^2$ $f_2 = \cos(0.5x_1\pi) \cos(0.5x_2\pi) + \frac{2}{ J_2 } \sum_{j \in J_2} \left(x_j - 2x_2 \sin\left(2\pi x_1 + \frac{j\pi}{n}\right) \right)^2$ $f_3 = \sin(0.5x_1\pi) + \frac{2}{ J_3 } \sum_{j \in J_3} \left(x_j - 2x_2 \sin\left(2\pi x_1 + \frac{j\pi}{n}\right) \right)^2$ <p>J_1, J_2, and J_3 are the same as those of UF10</p>	<p>UF10:</p> $f_1 = \cos(0.5x_1\pi) \cos(0.5x_2\pi) + \frac{2}{ J_1 } \sum_{j \in J_1} (4y_j - \cos(8\pi y_j + 1))$ $f_2 = \cos(0.5x_1\pi) \cos(0.5x_2\pi) + \frac{2}{ J_1 } \sum_{j \in J_2} (4y_j - \cos(8\pi y_j + 1))$ $f_3 = \cos(0.5x_1\pi) + \frac{2}{ J_3 } \sum_{j \in J_3} (4y_j - \cos(8\pi y_j + 1))$ <p>$J_1 = \{j 3 \leq j \leq n \text{ and } j - 1 \text{ is a multiplication of } 3\}$ $J_2 = \{j 3 \leq j \leq n \text{ and } j - 2 \text{ is a multiplication of } 3\}$ $J_3 = \{j 3 \leq j \leq n \text{ and } j - 3 \text{ is a multiplication of } 3\}$</p>	

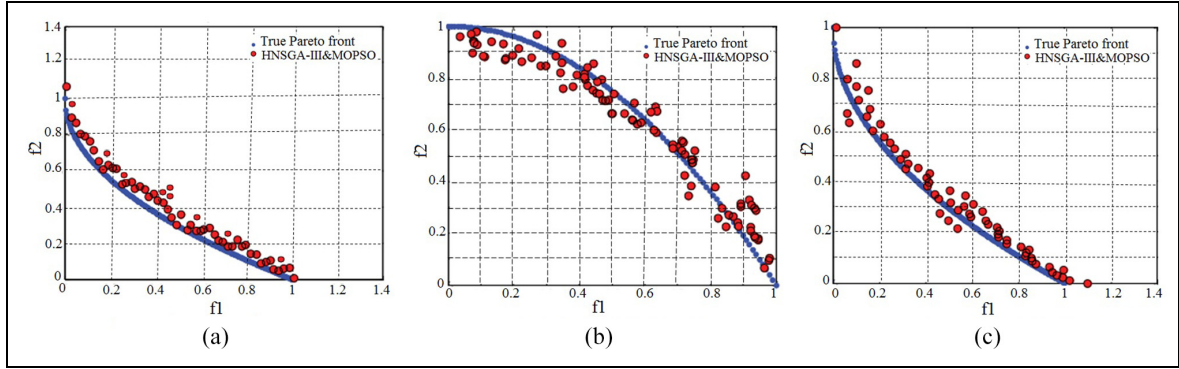


Figure 5. Pareto front of bi-objective benchmark functions: Pareto front of (a) UF2 functions, (b) UF4 functions, and (c) UF5 functions.

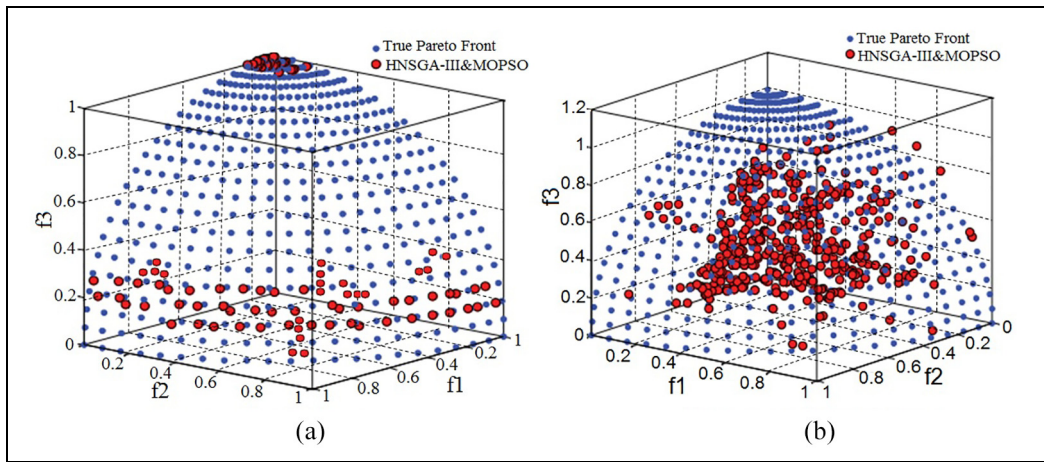


Figure 6. Pareto front of tri-objective benchmark functions: Pareto front of (a) UF8 functions and (b) UF10 functions.

$$SP = \sqrt{\frac{1}{N-1} \sum_{i=1}^{N-1} (\bar{d} - d_i)^2} \quad (2)$$

where \bar{d} is the average of all d_i , N is the number of Pareto optimal solutions obtained, and

$$d_i = \min (|f_1^i(x) - f_1^j(x)| + |f_1^i(x) - f_2^j(x)|) \\ \text{for all } i, j = 1, 2, 3, \dots, N$$

$$MS = \sqrt{\sum_{i=1}^M \max [d(a_i, b_i)]} \quad (3)$$

where d is a function to calculate the Euclidean distance, b_i is the minimum in the i th objective, and M is the number of objectives.

In addition to using performance metrics, the best Pareto optimization set that HNSGA-III&MOPSO obtained on both parameter space and search space is shown in Figures 5 and 6. These figures show the

Table 2. NSGA-III algorithm parameters.

Maximum number of iterations	MaxIt = 10,000
Population size	nPop = 100
Crossover percentage	pCrossover = 0.5
Mutation percentage	pMutation = 0.5
Mutation rate = 0.02	mu = 0.02
Number of parnets (offsprings)	nCrossover = 2*round(pCrossover*nPop/2)
Number of mutants	nMutation = round(pMutation*nPop)
Mutation step size	sigma = 0.1*(VarMax - VarMin)
Generating reference points	nDivision = 10 Zr = GenerateReferencePoints(nObj, nDivision)

performance of HNSGA-III&MOPSO compared to the real Pareto front. To evaluate comparisons, all algorithms are run 20 times for test problems and the statistical results of 20 runs and algorithm parameters are provided in Tables 2–4. Statistical results of the algorithm for IGD, SP, and MS are provided, respectively,

Table 3. MOPSO algorithm parameters.

Maximum number of iterations	MaxIt = 10,000	Inertia weight damping rate	wdamp = 0.99
Population size	nPop = 100	Personal learning coefficient	c1 = 1
Deletion selection pressure	gamma = 2	Global learning coefficient	c2 = 2
Mutation rate	mu = 0.1	Number of grids per dimension	nGrid = 7
Leader selection pressure	beta = 2	Inflation rate	alpha = 0.1
Repository size	nRep = nPop/2	Inertia weight	w = 0.5

Table 4. HNSGA-III&MOPSO algorithm parameters.

Maximum number of iterations	MaxIt = 10,000	Inertia weight damping rate	wdamp = 0.99
Population size	nPop = 100	Personal learning coefficient	c1 = 1
Mutation percentage	pMutation = 0.5	Global learning coefficient	c2 = 2
Mutation rate = 0.02	mu = 0.02	Number of grids per dimension	nGrid = 7
Crossover percentage	pCrossover = 0.5	Inflation rate	alpha = 0.1
Repository size	nRep = nPop/2	Leader selection pressure	beta = 2
Inertia weight	w = 0.5	Deletion Selection Pressure	gamma = 2
Generating reference points	nDivision = 10	Mutation rate	mu = 0.1

Table 5. Results for IGD.

IGD	UF2					UF4				
	Average	Median	Std. dev.	Worst	Best	Average	Median	Std. dev.	Worst	Best
MOPO	0.0714	0.04536	0.03752	0.14551	0.03632	0.13453	0.14432	0.00636	0.15485	0.12335
NSGA-III	0.12244	0.1242	0.01243	0.14485	0.10454	0.06823	0.06835	0.00254	0.07078	0.06424
HNSGA-III&MOPSO	0.01362	0.01555	0.00269	0.01445	0.01260	0.02634	0.02815	0.00168	0.02777	0.02289
IGD	UF5					UF8				
	Average	Median	Std. dev.	Worst	Best	Average	Median	Std. dev.	Worst	Best
MOPSO	2.50638	2.42504	0.57004	3.03533	1.48659	0.56681	0.53667	0.28667	0.69647	0.28530
NSGA-III	1.26755	1.33741	0.13839	1.46735	0.12145	0.56681	0.53667	0.28667	0.69647	0.28530
HNSGA-III&MOPSO	0.47889	0.45400	0.08469	0.53541	0.22341	0.19659	0.27840	0.06717	0.33488	0.17553
IGD	UF10									
	Average	Median	Std. dev.	Worst	Best					
MOPSO										
NSGA-III	1.63529	1.59123	0.29349	2.16232	1.22048					
HNSGA-III&MOPSO	1.70324	1.54323	0.55133	3.03835	1.13806					

IGD: Inverted Generational Distance; MOPSO: multi-objective particle swarm optimization.

In Tables 5–7, IGD shows that the proposed hybrid algorithm (HNSGA-III&MOPSO) can provide the best results on all statistics for issues that test two goals. IGD is a performance indicator that shows the accuracy and convergence of the algorithm. Therefore, it can be said that the proposed HNSGA-III&MOPSO algorithm can provide outstanding convergence on benchmarking two or three optimal goals. Pareto optimal solution

results of HNSGA-III&MOPSO on each benchmark are also described in Figures 5 and 6.

The resulting Pareto front is shown in Figures 6 and 7.

The numerical results prove that HNSGA-III&MOPSO having good performance for optimal objects is two objects; it relates to the convergence and scope of the search. However, HNSGA-III&MOPSO

Table 6. Results for SP.

SP	UF2					UF4				
	Average	Median	Std. dev.	Worst	Best	Average	Median	Std. dev.	Worst	Best
MOPSO	0.00849	0.00834	0.00168	0.01245	0.00624	0.00666	0.00672	0.00081	0.00819	0.00557
NSGA-III	0.00866	0.00879	0.00096	0.01042	0.00797	0.00780	0.00758	0.00066	0.00876	0.00617
HNSGA-III&MOPSO	0.02730	0.02624	0.01259	0.06499	0.01740	0.02843	0.02886	0.00465	0.03784	0.02038
SP	UF5					UF8				
	Average	Median	Std. dev.	Worst	Best	Average	Median	Std. dev.	Worst	Best
MOPSO	0.00456	0.00487	0.00408	0.01206	0.00006					
NSGA-III	0.00278	0.00007	0.00553	0.01665	0.00001	0.02692	0.02737	0.00867	0.04453	0.01731
HNSGA-III&MOPSO	0.12545	0.12738	0.03505	0.16826	0.7467	0.24374	0.23799	0.03889	0.28492	0.16359
SP	UF10									
	Average	Median	Std. dev.	Worst	Best					
MOPSO										
NSGA-III	0.01984	0.02064	0.00378	0.02645	0.01538					
HNSGA-III&MOPSO	1.06778	0.89534	0.41961	1.81768	0.67319					

SP: Spacing; MOPSO: multi-objective particle swarm optimization.

Table 7. Results for MS.

MS	UF2					UF4				
	Average	Median	Std. dev.	Worst	Best	Average	Median	Std. dev.	Worst	Best
MOPSO	0.91505	0.91836	0.02460	0.86676	0.95651	0.81545	0.81344	0.01557	0.75441	0.83449
NSGA-III	0.87501	0.87337	0.00580	0.85436	0.87884	0.88564	0.88431	0.01866	0.84324	0.91394
HNSGA-III&MOPSO	0.89262	0.88368	0.05465	0.82235	0.93863	0.95766	0.96653	0.01532	0.92242	0.95666
MS	UF5					UF8				
	Average	Median	Std. dev.	Worst	Best	Average	Median	Std. dev.	Worst	Best
MOPSO	0.23923	0.28663	0.09845	0.15784	0.43677					
NSGA-III	0.29341	0.29565	0.3560	0.23544	0.34550	0.55310	0.54401	0.16736	0.26523	0.71676
HNSGA-III&MOPSO	0.82346	0.83676	0.06766	0.64314	0.95436	0.34398	0.36783	0.47428	0.27879	0.77412
MS	UF10									
	Average	Median	Std. dev.	Worst	Best					
MOPSO										
NSGA-III	0.13435	0.10433	0.06253	0.06679	0.25414					
HNSGA-III&MOPSO	0.24643	0.14474	0.38569	0.03383	0.96133					

MS: Maximum Spread; MOPSO: multi-objective particle swarm optimization.

having good performance for optimal objects is three objects; the proposed algorithm shows high convergence and better coverage of many MOPSO and NSGA-III algorithms. From here, we can say that the

main advantages of the algorithm HNSGA-III&MOPSO proposed compared to NSGA-III and MOPSO are the convergence characteristics and the ability to search more broadly. In addition, the results

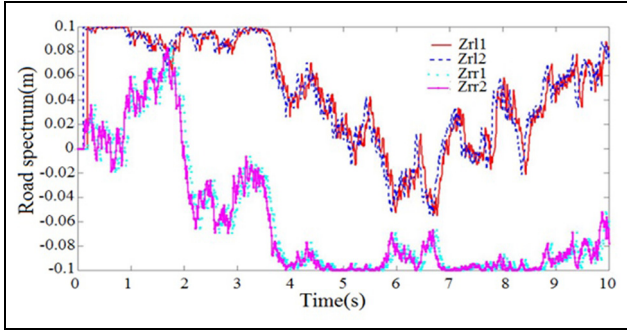


Figure 7. Road surface profiles.

of HNSGA-III&MOPSO are proposed in most cases better than MOPSO and NSGA-III. Therefore, the results show that HNSGA-III&MOPSO is proposed to outperform MOPSO and NSGA-III because it uses a combination of search operators of both algorithms to create a new population. In addition, the MOPSO algorithm updates the $gBest$ in each iteration. Therefore, all particles are attracted by the same or a similar $gBest$ (i) group in each iteration, while individuals of HNSGA-III&MOPSO are updated for each generation, thus supporting assist search agents to explore a wider search space. This proves that the hybrid method has actually been successful. It gives more accurate results and less search time than the other two algorithms.

Vibration characteristic of the Powertrain mount system

Mathematical model: Full car model with 10 degrees of freedom (DOF) is shown in Figure 1. Suspension and tires are considered spring and damping systems. Where the masses $m_{2,1}$, $m_{2,2}$, $m_{2,3}$, and $m_{2,4}$ denote the weight of four wheels (the mass does not burst). The masses m_{cg1} and m_{cab} represent the mass (unburnt mass) of the frame and electric motor, respectively. $Z_{3,1}$, $Z_{3,2}$, $Z_{3,3}$, $Z_{3,4}$ are the vertical displacements of the wheel; Z_1 , Z_2 are, respectively, the vertical displacement of the frame and the transmission system. And, Roll and Altitude are vibrations that rotate around the corresponding X and Y axes. Next, the symbol Φ and Ψ represent the pitch and roll of the frame. The inertia of the transmission system on the y -axis and the x -axis are I_{yy} and I_{xx} , respectively; the inertial moment for the chassis on axes $X1$ and $Y1$ are I_{yy1} and I_{xx1} , respectively. The stiffness and damping parameters of the wheels are $K_{3,1}$, $K_{3,2}$, $K_{3,3}$, $K_{3,4}$ and $C_{3,1}$, $C_{3,2}$, $C_{3,3}$, $C_{3,4}$, respectively. Similarly, the hardness and damping parameters of primary suspension are $K_{2,1}$, $K_{2,2}$, $K_{2,3}$, $K_{2,4}$ and $C_{2,1}$, $C_{2,2}$, $C_{2,3}$, $C_{2,4}$, respectively, while the hardness and damping parameters of

Table 8. Parameters of the mathematical model.

Symbol	Parameters of the mathematical model
X_i	Vector column of displacements and angular oscillations of masses
M	The matrix of inertial coefficients of car parts
C	The matrix of coefficients of stiffnesses and torsional rigidity
K	The matrix of damping coefficients
$Q(t)$	Column vector of the perturbing forces and moments
q_1, q_2	Universal road surface amplitude at front and rear wheels
	$q_2(t) = q_1(t + \tau)$ with τ : time interval, v : vehicle speed

the drive system are $K_{1,1}$, $K_{1,2}$, $K_{1,3}$ and $C_{1,1}$, $C_{1,2}$, $C_{1,3}$, respectively. The distance of the front and rear support from the center (CG) of the transmission system is a and b , respectively; the right and left mounting distances from the CG of the transmission system are c and d , respectively. $a1$, $b1$ and $c1$, $d1$ are the distances for the chassis.

Using Newton's law, the mathematical model of Figure 1 can be written as follows

$$M\ddot{x}_i + K\dot{x}_i + Cx_i = Q(t) \quad (4)$$

where the symbols are shown in Table 8.

Multi-objective optimization functions

There are many indicators to evaluate the vibration of the Powertrain. In particular, mean square acceleration oscillates at the front and rear of the Powertrain mount, the mean square displacement difference between the Powertrain and vehicle chassis at the front and rear Powertrain mount. These are two important parameters that determine the decisive influence of unit Powertrain vibration on chassis. In order to optimally reduce the vibration of the unit Powertrain, we need to simultaneously optimize the parameters of mean square acceleration and mean square displacement at the front and rear, right and left of the Powertrain mounts.

The average square value of the vibration acceleration of any points can be determined by the following formula

$$\ddot{z} = \sqrt{\int_{-\infty}^{\infty} S_z(\omega) d\omega} = \sqrt{\int_{-\infty}^{\infty} \omega^4 |W_z(j\omega)|^2 S_q(\omega) d\omega} \quad (5)$$

where ω is the frequency, $|W_z(j\omega)|^2$ is the squared modulus of amplitude and phase characteristics, and $S_q(\omega)$ is the spectral density of exposure.

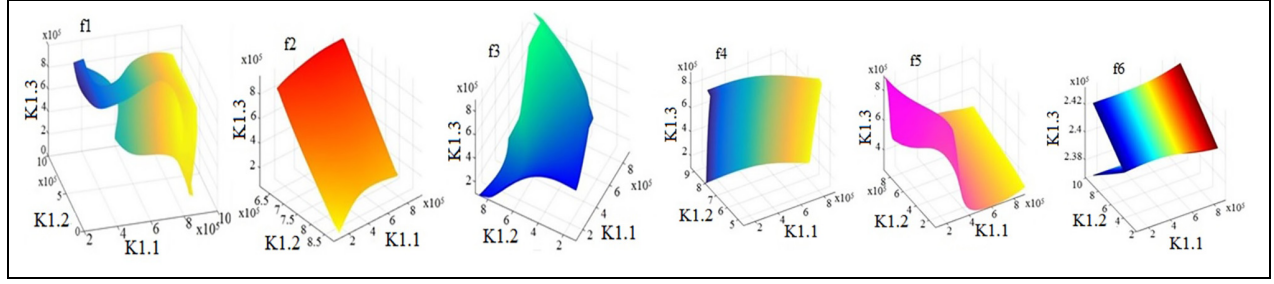


Figure 8. Values of six-objective optimization functions.

The modules of the amplitude and phase characteristics of the vibratory displacement of the Powertrain and the car body in the place of the front mount are

$$W_k^{O_1}(j\omega) = W_0(j\omega) + W_0^\phi(j\omega) \cdot l_3 \quad (6)$$

$$W_{ca}^{O_1}(j\omega) = W_{ca}^\phi(j\omega) + W_{ca}(j\omega) \cdot l_6 \quad (7)$$

where $W_0(j\omega)$ is the module amplitude–phase characteristics in the center of the car body, $W_0^\phi(j\omega)$ is the module amplitude–phase characteristics of the longitudinal-angular body of the car, $W_k^{O_1}(j\omega)$ is the module of the amplitude and phase characteristics of the body in place of the front mount of the Powertrain, $W_{ca}(j\omega)$ is the module amplitude–phase characteristics in the center of the Powertrain of the car, $W_{ca}^\phi(j\omega)$ is the module amplitude–phase characteristics of the longitudinal-angular Powertrain of the car, and $W_{ca}^{O_1}(j\omega)$ is the modulus of amplitude–phase characteristics in place of the front mount of the Powertrain.

The modules of the amplitude–phase characteristics of the vibration displacement of the Powertrain and the car body in the place of the rear mount are

$$W_k^{O_2}(j\omega) = W_0(j\omega) + W_0^\phi(j\omega) \cdot l_4 \quad (8)$$

$$W_{ca}^{O_2}(j\omega) = W_{ca}(j\omega) - W_{ca}^\phi(j\omega) \cdot l_7 \quad (9)$$

where $W_k^{O_2}(j\omega)$ is the module of the amplitude–phase characteristics of the body in the place of the rear mount of the Powertrain and $W_{ca}^{O_2}(j\omega)$ is the module of amplitude–phase characteristics in the place of the rear mount of the Powertrain.

The difference of the module frequency response of the vibration of the Powertrain and the car body in place of the front mount of the Powertrain is

$$W_{ca-k}^{O_1}(j\omega) = W_{ca}^{O_1}(j\omega) - W_k^{O_1}(j\omega) \quad (10)$$

The difference of the frequency response module of the vibration displacement of the Powertrain and the car body at the rear mount is

Table 9. Model parameters.

No.	Parameter	Value	Unit
1	$m_{2.1}, m_{2.2}, m_{2.3}, m_{2.4}$	60	kg
2	m_{cab}, m_{cg1}	1000, 1200	kg
3	$K2.1, K2.2, K2.3, K2.4$	37,000	N m
4	$C2.1, C2.2, C2.3, C2.4$	700	N s/m
5	$K3.1, K3.2, K3.3, K3.4$	55,000	N m
6	$C3.1, C3.2, C3.3, C3.4$	4000	N s/m
7	$K1.1, K1.2, K1.3$	670,000	N m
8	$C1.1, C1.2, C1.3$	6000	N s/m
9	$a, b, c = d$	0.187, 0.623, 0.3	m
10	$a1 = b1, c1 = d1$	1.5, 1	m
11	lxx, lyy	320, 80	Kg m ²
12	$lxx1, lyy1$	4000, 950	Kg m ²

$$W_{ca-k}^{O_2}(j\omega) = W_{ca}^{O_2}(j\omega) - W_k^{O_2}(j\omega) \quad (11)$$

Simulated input parameters

Road surface profiles. When the vehicle moves, there are many factors that cause the vibration:: the internal force in the car; external forces that appear in the process of using acceleration, braking, and revolving; exterior conditions such as wind and storm; and boring face street. Among the factors on the bumpy side of the road is the oscillation cause of the vehicle. To simulate the most general calculation, we use the road surface profile as a random function as in Figure 7 and simulated parameters as shown in Table 9.

Simulation results of application HNSGA-III&MOPSO method to optimization of the Powertrain mount system stiffness parameter

Through Matlab, we calculated six functions of acceleration and displacement according to the stiffnesses of the front left, front right, and rear Powertrain mount ($K1.1, K1.2, K1.3$) value as shown in Figure 8 (Figures 8–10 show the results in the form of 4D—four-dimensional space via the Isosurfaces function in Matlab).

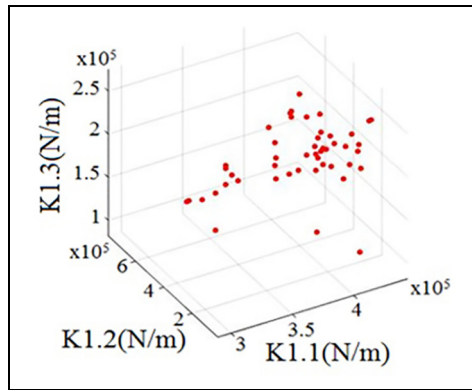


Figure 9. Pareto front of the solutions after 1000 generations, 200 population.

Values of six-objective optimization functions according to the stiffnesses ($K1.1$, $K1.2$, $K1.3$): $f1$ is MSD at the front left Powertrain mount, $f2$ is MSA at the front left Powertrain mount, $f3$ is MSD at the front right Powertrain mount, $f4$ is MSA at the front right Powertrain mount, $f5$ is MSD at the rear Powertrain mount, and $f6$ is MSA at the rear Powertrain mount.

It is well known that the results of multi-objective optimization would be a set of non-dominated optimized points called Pareto set. These points offer a wide range of parameters to the designer to choose the optimum point depending on his designing conditions. There are always conflicting objective functions in vehicle designing where improvement in one function may have an unfavorable influence on other functions. In this article, multi-objective optimization for all six-objective functions is done simultaneously. Application of HNSGA-III&MOPSO optimization algorithm: we obtain results as shown in Figures 9 and 10:

The average square of the Pareto front of MSD at the front left Powertrain mount: $f1 = 4.1258e-05$ (m).
 The average square of the Pareto front of MSA at the front left Powertrain mount: $f2 = 1.5962$ (m/s^2).
 The average square of the Pareto front of MSD at the front right Powertrain mount: $f3 = 5.5557e-05$ (m).

The average square of the Pareto front of MSA at the front right Powertrain mount: $f4 = 1.8014$ (m/s^2).

The average square of the Pareto front of MSD at the rear Powertrain mount: $f5 = 2.2680e-05$ (m).

The average square of the Pareto front of MSA at the rear Powertrain mount: $f6 = 1.3224$ (m/s^2).

In which $f1$ is the Pareto front of MSD at the front left Powertrain mount, $f2$ is the Pareto front of MSA at the front left Powertrain mount, $f3$ is the Pareto front of MSD at the front right Powertrain mount, $f4$ is the Pareto front of MSA at the front right Powertrain mount, $f5$ is the Pareto front of MSD at the rear Powertrain mount, and $f6$ is the Pareto front of MSA at the rear Powertrain mount.

Application of HNSGA-III&MOPSO optimization algorithm with 6-objective functions ($f1$, $f2$, $f3$, $f4$, $f5$, $f6$): the red dots on $f2$, $f3$, $f5$, $f6$ and the blue dots on $f1$, $f4$ are the result set of the Pareto front that the HNSGA-III&MOPSO algorithm has found.

HNSGA-III&MOPSO has been applied in the problem of Powertrain mount system stiffness parameters optimization. Simulation results comparing one of the results in the set of the Pareto front from the HNSGA-III&MOPSO algorithm with different stiffness values ($K1.1$, $K1.2$, $K1.3$) are shown in Figures 11 and 12.

Figure 11 shows the acceleration of the vehicle frame corresponding to the different stiffness values. Symbol A corresponds to the optimal stiffness value in a set of the Pareto front. Symbol B corresponds to $K1.1 = 290,000$, $K1.2 = 350,000$, $K1.3 = 550,000$. Symbol C corresponds to $K1.1 = 790,000$, $K1.2 = 750,000$, $K1.3 = 350,000$. From the graph, we see that the smallest acceleration is at the optimal stiffness value.

Similarly, Figure 12 shows the displacement of the vehicle frame corresponding to the different stiffness values. Symbol A1 corresponds to the optimal stiffness value in a set of the Pareto front. Symbol A2 corresponds to $K1.1 = 290,000$, $K1.2 = 350,000$, $K1.3 = 750,000$. Symbol A3 corresponds to $K1.1 = 790,000$, $K1.2 = 750,000$, $K1.3 = 650,000$. From the graph, we see that the smallest displacement is at the optimal stiffness value in a set of the Pareto front.

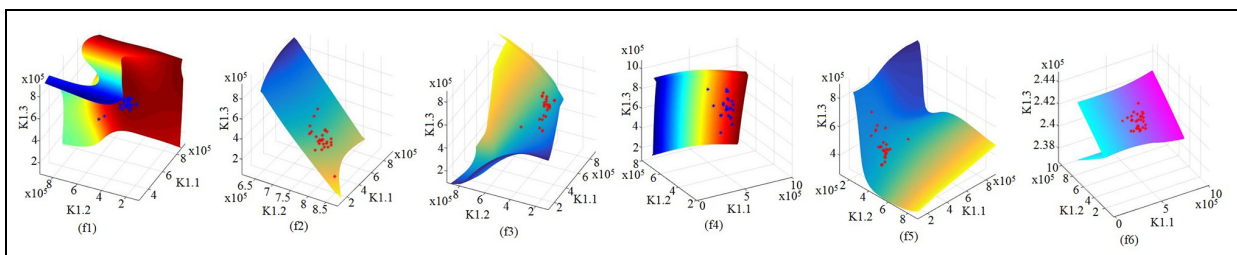


Figure 10. Global Pareto front of six-objective optimization functions.

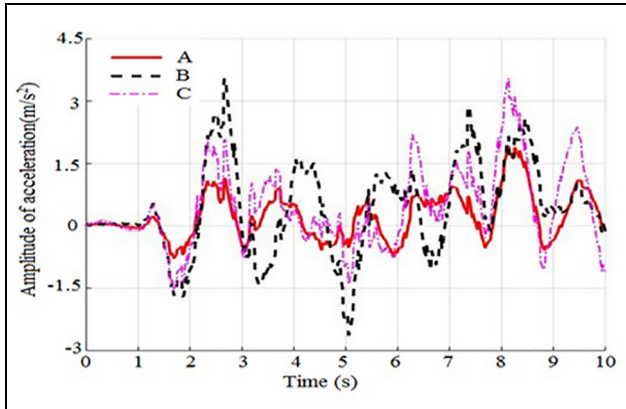


Figure 11. Acceleration of the vehicle frame.

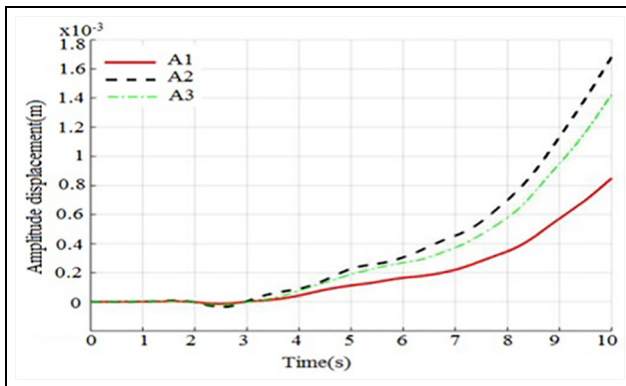


Figure 12. Displacement of the vehicle frame.

Conclusion

The combination of the MOPSO algorithm and the genetic algorithm NSGA-III has been implemented in this article. The results of this technique find the globally optimal set of multi-object problems. The hybrid method HNSGA-III&MOPSO has been rated high performance, which has been assessed through a series of comparative testing methods for benchmarking two goals or three goals. In addition, these results are compared with other multi-purpose optimization methods such as MOPSO and NSGA-III. The numerical results demonstrate that this new hybrid algorithm is more effective in solving multi-objective optimization problems with many possibilities for convergence and search.

The amplitude of the acceleration of the vehicle frame decreased by 22.8%, and the amplitude of the displacement of the vehicle frame reduced by 12.4% compared to the normal design case. The calculation time of the algorithm HNSGA-III&MOPSO is less than the algorithm NSGA-III, that is, 5 and 6 h, respectively, compared to the algorithm MOPSO.


Declaration of conflicting interests

The author(s) declared no potential conflicts of interest with respect to the research, authorship, and/or publication of this article.

Funding

The author(s) disclosed receipt of the following financial support for the research, authorship, and/or publication of this article: This work was supported by VIETNAM TNK CONSULTANT & SERVICE COMPANY LIMITED (0107487266).

ORCID iD

Dinh-Nam Dao  <https://orcid.org/0000-0001-9810-2096>

References

- Jeong T and Singh R. Analytical methods of decoupling the automotive engine torque roll axis. *J Sound Vibrat* 2000; 234: 85–114.
- Park J-Y and Singh R. Effect of non-proportional damping on the torque roll axis decoupling of an engine mounting system. *J Sound Vibrat* 2008; 313: 841–857.
- Hu J-F and Singh R. Improved torque roll axis decoupling axiom for a Powertrain mounting system in the presence of a compliant base. *J Sound Vibrat* 2012; 331: 1498–1518.
- Yu Y, Naganathan NG and Dukkipati RV. A literature review of automotive vehicle engine mounting systems. *Mech Mach Theory* 2001; 36: 123–142.
- Adiguna H, Tiwari M, Singh R, et al. Transient response of a hydraulic engine mount. *J Sound Vibrat* 2003; 268: 217–248.
- Konak A, Coit D and Smith A. Multi-objective optimization using genetic algorithms: a tutorial. *Reliabil Eng Syst Safety* 2006; 91: 92–107.
- Deb K, Pratap A, Agarwal S, et al. A fast elitist multi-objective genetic algorithm: NSGA-II. *IEEE Trans Evol Computat* 2002; 6: 182–197.
- Chang L-C and Chang F-J. Multi-objective evolutionary algorithm for operating parallel reservoir system. *J Hydrol* 2009; 377: 12–20.
- Ishibuchi H, Tsukamoto N and Nojima Y. Evolutionary many-objective optimization: a short review. In: *Proceedings of IEEE congress on evolutionary computation*, Hong Kong, China, 1–6 June 2008, pp.1–6. New York: IEEE.
- Malekmohammadi B, Zahraie B and Kerachian R. A ranking solution of multi-objective reservoir operation optimization models using multi-criteria decision analysis. *Expert Syst Appl* 2011; 38: 7851–7863.
- Deb K and Jain H. Handling many-objective problems using an improved NSGA-II procedure. In: *Proceedings of IEEE congress on evolutionary computation (CEC)*, Brisbane, QLD, Australia, 10–15 June 2012. New York: IEEE.
- Deb K and Jain H. An evolutionary many objective optimization algorithms using reference-point based non-

- dominated sorting approach, part I: solving problems with box constraints. *IEEE Trans Evol Computat* 2014; 18: 577–601.
13. Coello CAC, Pulido GT and Lechuga MS. Handling multiple objectives with particle swarm optimization. *IEEE Trans Evol Comput* 2004; 8: 256–279.
 14. Zhang Q and Li H. MOEA/D: a multi-objective evolutionary algorithm based on decomposition. *IEEE Trans Evol Comput* 2007; 11: 712–731.
 15. Coello CAC and Lechuga MS. MOPSO: a proposal for multi-objective swarm optimization. *Evol Comput* 2002; 2: 1051–1056.
 16. Baltar AM and Fontane DG. A multi-objective particle swarm optimization model for reservoir operations and planning. In: *Proceedings of joint international conference on computing and decision making in civil and building engineering*, Montréal, QC, Canada, 14–16 June 2006, pp.1–16.
 17. Baltar AM and Fontane DG. A generalized multiobjective particle swarm optimization solver for spreadsheet models: application to water quality. In: *Proceedings of hydrology days*, Fort Collins, CO, 7–8 March 2006, pp.1–12. Fort Collins, CO: Colorado State University.
 18. Reddy MJ and Kumar DN. Multi-objective particle swarm optimization for generating optimal trade-offs in reservoir operation. *Hydrol Process* 2007; 21: 2897–2909.
 19. Reddy MJ and Kumar DN. Performance evaluation of elitist-mutated multi-objective particle swarm optimization for integrated water resources management. *J Hydroinformat* 2009; 11: 79–88.
 20. Wang S, Huang X and Lei X. Multi-objective optimization of reservoir flood dispatch based on MOPSO algorithm. In: *Proceedings of 8th international conference on natural computation*, Chongqing, China, 29–31 May 2012, pp.29–31.
 21. Mirjalili S, Saremi S, Mirjalili MS, et al. Multi-objective grey wolf optimizer: a novel algorithm for multi-criterion optimization. *Expert Syst Appl* 2016; 47: 106–119.
 22. Pradhan PM and Panda G. Solving multi-objective problems using cat swarm optimization. *Expert Syst Appl* 2012; 39: 2956–2964.
 23. Velazquez JMO and Coello CAC Arias-Montano A. Multi-objective compact differential evolution. In *2014 IEEE symposium on differential evolution*, Orlando, FL, 19–12 December 2014, pp.1–8. New York: IEEE.
 24. Hemmatian H, Fereidoon A and Assareh E. Optimization of hybrid laminated composites using the multi-objective gravitational search algorithm (MOGSA). *Eng Optim* 2014; 46: 1169–1182.
 25. Shi X and Kong D. A multi-objective ant colony optimization algorithm based on elitist selection strategy. *Metalurg Mining Ind* 2015; 7: 333–338.
 26. Hancer E, Xue B, Zhang M, et al. A multi-objective artificial bee colony approach to feature selection using fuzzy mutual information. In: *2015 IEEE congress on evolutionary computation (CEC)*, Sendai, Japan, 25–28 May 2015, pp.2420–2427. New York: IEEE.
 27. Lin W, Yu D, Zhang C, et al. A multi-objective teaching-learning-based optimization algorithm to scheduling in turning processes for minimizing makespan and carbon footprint. *Production* 2015; 101: 337–347.
 28. Jeong S, Hasegawa S, Shimoyama K, et al. Development and investigation of efficient GA/PSO-hybrid algorithm applicable to real-world design optimization. In: *IEEE congress on evolutionary computation*, Trondheim, 18–21 May 2009. New York: IEEE.
 29. Premalatha K and Natarajan AM. Hybrid PSO and GA for global maximization. *Int J Open Problems Comp* 2009; 2: 597–608.
 30. Bai H-B. An improved multi-objective particle swarm optimization. *Int J Comp Optimizat* 2016; 3: 105–120.
 31. Pourtakdoust SH and Zandavi SM. A hybrid simplex non-dominated sorting genetic algorithm for multiobjective optimization. *Int J Swarm Intel Evol Comput* 2016; 5: 3.
 32. Yang G, Xu T, XLI, et al. An efficient hybrid algorithm for multiobjective optimization problems with upper and lower bounds in engineering. *Mathemat Prob Eng* 2015; 2015: 932029.
 33. Rashidi E, Jahandar M and Zandieh M. An improved hybrid multi-objective parallel genetic algorithm for hybrid flow shop scheduling with unrelated parallel machines. *Int J Adv Manufact Tech* 2010; 49: 1129–1139.
 34. Kennedy J, Kennedy JF, Eberhart RC, et al. *Swarm intelligence* (The Morgan Kaufmann series in evolutionary computation). Burlington, MA: Morgan Kaufmann; 2001, pp.81–86.
 35. Bo Z and Cao YJ. Multiple objective particle swarm optimization techniques for economic load dispatch. *J Zhejiang Univ Sci* 2005; 6: 420–427.
 36. Li CF, Zhu QX and Geng ZQ. Multi-objective particle swarm optimization hybrid algorithm: an application on the industrial cracking furnace. *Ind Eng Chem Res* 2007; 46: 3602–3609.
 37. Kitamura S, Mori K, Shindo S, et al. Modified multiobjective particle swarm optimization method and its application to energy management system for factories. *IEEJ Trans Electr Informat Syst* 2005; 125: 21–28.
 38. Zhang Q, Zhou A and Zhao S. *Multi-objective optimization test instances for the CEC 2009 special session and competition*. Colchester: University of Essex, 2008, pp.1–30.
 39. Schott JR. *Fault tolerant design using single and multi-criteria genetic algorithm optimization*. Cambridge, MA: Department of Aeronautics and Astronautics, Massachusetts Institute of Technology, 1995, pp.199–200.
 40. Zitzler E and Thiele L. Multi-objective evolutionary algorithms: a comparative case study and the strength Pareto approach. *Evol Comput IEEE Trans* 1999; 3: 257–271.